

An Effect of Downcomer Feedwater Fraction on Steam Generator Performance with an Axial Flow Economizer

Byung Ryul Jung, Hu Shin Park, Duk Muk Chung and Se Jin Baik

Korea Power Engineering Company, Inc.
Taejon, Korea 305-353

Abstract

The effects of feedwater flow fraction introduced into the downcomer region have been evaluated in terms of steam generator performance based on the same steam generator thermal output for the Korea Standard Nuclear Power Plant (KSNP) steam generator. The KSNP steam generator design has an integral axial flow economizer which is designed such that most of the feedwater is introduced through the economizer region and only a portion of feedwater through the downcomer region. The feedwater flow introduced into the downcomer region is not normally controlled during the power operation. However, the actual feedwater fraction into the downcomer region may differ from the design flow depending on the as-built system and component characteristics. Investigated in this paper were the downcomer feedwater flow effects on the steam pressure, circulation ratio, internal void fraction and velocity distribution in the tube bundle region at the steady state operation using SAFE and ATHOS3 codes. The results show that the steam pressure increases and the resultant total feedwater flow increases with reducing the downcomer feedwater flow fraction for the same steam generator thermal output. The slight off-design condition of downcomer feedwater flow fraction renders no significant effect on the steam generator performance such as circulation ratios, steam qualities, void fractions and internal velocity distributions. The evaluation shows that the slight off-design downcomer feedwater flow fraction deviation up to $\pm 5\%$ is acceptable for the steam generator performance.

1. Introduction

The Korea Standard Nuclear Power Plant (KSNP) steam generator design is of the similar type as CENP System80 steam generators. The KSNP steam generator is a recirculating U-tube design with an integral axial flow economizer where feedwater is introduced through two feedwater nozzles near the bottom of the cold leg evaporator into a distribution box and through the downcomer nozzle near the top of the downcomer. The economizer is defined by a semi-cylindrical section of the tube bundle region above the tubesheet on the cold leg side. The economizer distribution box blocks the saturated recirculating water from the economizer section and provides feedwater to the cold leg tube bundle region at the surface of the tubesheet. The feedwater injection system is designed such that most of feedwater (typically 90% of the total feedwater flow) for KSNP is introduced through the economizer region above the tubesheet and only a portion of feedwater is introduced into the downcomer region through the downcomer nozzle.

Basically the downcomer feedwater flow path has two functions. The first one is to inject the cold emergency feedwater during certain transients, which is separate from the main feedwater flow path. The other one is to provide the main feedwater flow at low power level when the feedwater heater is not yet effective due to lack of turbine extraction steam. This precludes thermal shock to the pressure shell and economizer feedwater distribution box. The downcomer feedwater system, however, is utilized in an economizer steam generator design to provide a portion of feedwater during power operation to the downcomer region. A partial feed flow to the downcomer region reduces the feedwater control valve size in the flow path to the economizer region. This partial feed flow to the downcomer has another advantage that carryunder of steam in the recirculating fluid is quenched and a degree of subcooling is obtained in the downcomer. This increases circulation ratio slightly.

The feedwater flow fraction through the downcomer is set at approximately 10% of the total required feedwater flow during the power operation for the KSNP steam generator design. Not normally controlled is the feedwater flow introduced into the downcomer region during the power operation. The actual downcomer feedwater flow may, however, differ from that of the design flow depending on the as-built system and component characteristics. The effects of feedwater flow fraction between the economizer and the downcomer regions were evaluated in terms of steam generator performance based on the same steam generator thermal output. Specifically evaluated were the steam pressure, circulation ratios, internal void fractions, steam qualities and velocity distributions in the tube bundle region using the SAFE and ATHOS3 codes.

2. Analysis Method

To evaluate the downcomer feedwater fraction, 4 cases were analyzed with reducing downcomer feedwater fraction. The steam pressure was evaluated using the SAFE code and the results were used in the next ATHOS analyses.

The SAFE code has been used to size and analyze the performance of a steam generator that has an axial flow economizer. The SAFE code was used to estimate the feedwater flow fraction effect on the steam pressure. The estimated steam pressures were used in calculating the required total feedwater flow to maintain the same steam generator thermal output as the downcomer feedwater flow decreases. The steam pressure and the calculated feedwater flow were used for the ATHOS input.

The ATHOS3 code was used in evaluating the specific effects of the feedwater flow fraction. The ATHOS3 is a three-dimensional, two-phase, steady state and transient analysis code for thermal-hydraulic analysis of recirculating U-tube steam generators and has been used to analyze the thermal hydraulic performance for the KSNP steam generators. The code provides the detailed descriptions of steam generator secondary side velocities, pressure, temperature, and void fraction and the primary side and tube wall temperature fields.

The analyses were performed based on the KSNP steam generator design. The major steam generator design data are shown in Table 1. The steam generator nodalization used in the ATHOS3 analyses is shown in Figure 1. The steam generator is divided into 29 horizontal slabs. Due to geometric symmetry only half of the steam generator was modeled. Each half slab was divided into 10 radial concentric rings into 12 circumferential wedges.

The total feedwater flow input to the ATHOS3 analyses was calculated to maintain the same steam generator thermal output from the estimated steam generator pressure with the SAFE code. With this procedure, the primary to secondary heat input was maintained nearly the same for all analysis cases. Table 2 shows the major inputs for each case used in the ATHOS3 analyses.

Table 1. Referenced KSNP Steam Generator Design Data

Parameter	Value
Heat Load (Btu/hr)	4,824
Warranted Operating Steam Pressure (psia)	1,076
Total Feedwater Flow (lbm/hr)	6.36×10^6
Downcomer Feedwater Fraction (%)	10
Feedwater Temperature (°F)	450
Number of Tubes	8,214
Heat Transfer Area (ft ²)	62.46
Primary Mass Flow (lbm/hr)	60.75×10^6
Primary Inlet/Outlet Temperature (°F)	621.2 / 564.5
Primary Coolant Pressure (psia)	2,250

Table 2. ATHOS3 Analyses Input

	Case 1	Case 2**	Case 3	Case 4
Downcomer Feedwater Flow* (%)	15.0	10.0	5.1	0.1
Steam Pressure (psia)	1090.63	1094.13	1097.71	1101.35
Total Feedwater Flow (lbm/hr)	6.357	6.358	6.359	6.361
Feedwater Temperature (°F)	450	450	450	450
Primary Mass Flow (lbm/hr)	60.75×10^6	60.75×10^6	60.75×10^6	60.75×10^6
Thermal Output (Btu/hr)	4,824	4,824	4,824	4,824

* Fraction of feedwater introduced into downcomer region to total feedwater flow.

** Design case.

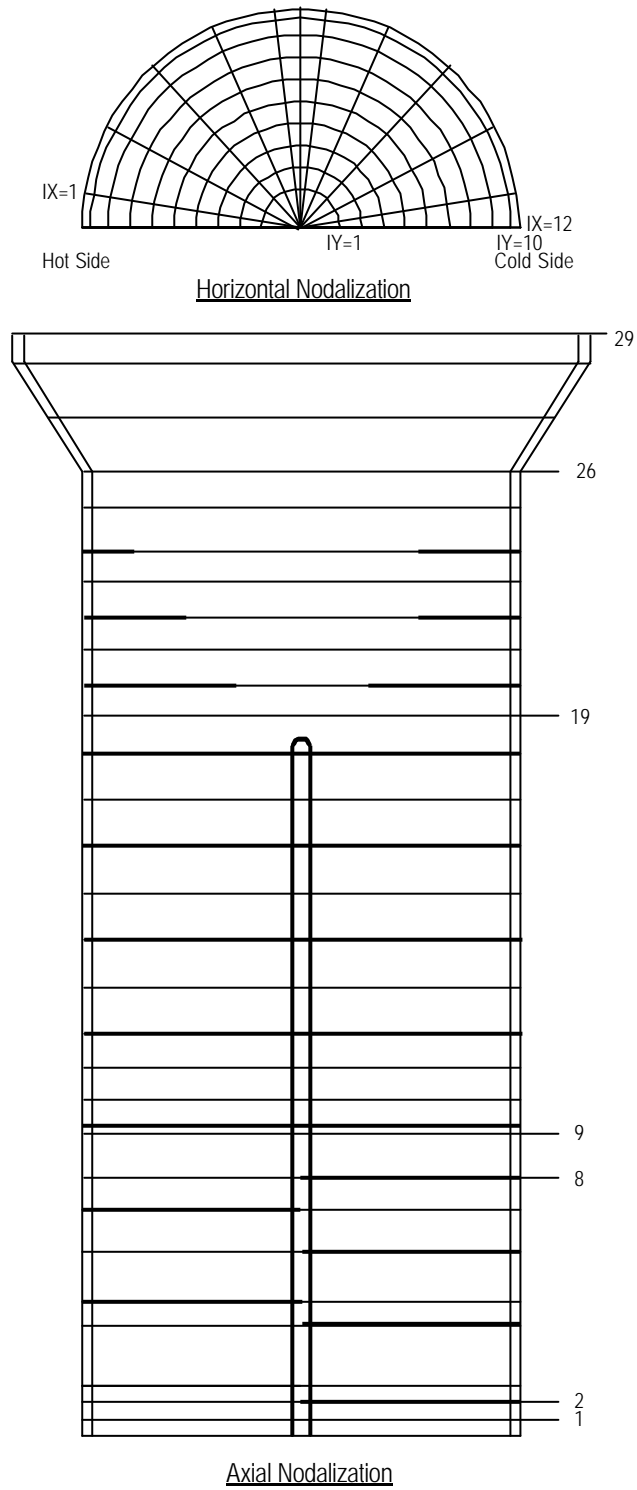


Figure 1. ATHOS3 Horizontal and Axial Nodalization

3. Results and Discussion

3.1 Steam Pressure

The SAFE code analysis result summary is shown in Table 3. The results show that relatively the less feedwater flow is introduced through the downcomer region, the higher steam pressure is attained. The maximum increase in steam pressure is about 7 psi for the nearly no downcomer feedwater flow case (Case 4). Due to the increase in the amount of preheated feedwater to saturated temperature in the economizer region, the heat transferred in the evaporator region slightly decreases but relatively more heat is available to evaporate the saturated liquid. For the same heat input, higher pressure is attained with more economizer feedwater flow and less latent heat of vaporization at higher pressure.

Table 3. SAFE Analyses Result Summary

	Case 1	Case 2	Case 3	Case 4
Downcomer Feedwater Flow* (%)	15.0	10.0	5.1	0.1
Steam Flow (lbm/hr)	6.357	6.358	6.359	6.361
Steam Pressure (psia)	1090.63	1094.13	1097.71	1101.35
Average Boiling Length (ft)	52.87	52.38	51.89	51.42
Overall Heat Transfer Coefficient (Btu/hr-ft ² -°F)	544.02	545.99	547.03	548.61
Boiling Region Heat Load** (%)	88.74	87.88	87.01	86.13
Pinch Point Heat Flux, q'' (Btu/hr-ft ²)	19.12	19.33	19.53	19.73
LMTD (°F)	88.02	87.78	87.53	87.28

* Fraction of feedwater introduced into downcomer region to total feedwater flow.

** Percentage of heat load in boiling region to total head load.

3.2. Circulation Ratio

In the natural recirculating steam generator, the ability to produce flow comes from the head available and the flow resistance in the flow circuit. The head available comes from the difference in densities of the fluids in the downcomer, evaporator and riser and their respective heights. It is important to keep carryunder of steam in the recirculating water to a minimum since uncondensed steam reduces the downcomer density and therefore the force available for circulation. However, the reduction in the driving force due to reduced downcomer water density is slightly offset and resultant circulation ratio is less decreased due to an increased fraction of forced flow in the economizer region with reducing the downcomer feedwater flow fraction.

The results show that the circulation ratio slightly decreases with reducing downcomer feedwater flow fraction based on the same steam generator thermal output. The maximum decrease in the overall circulation ratio is about 5.7 % of the design case in the almost no downcomer feedwater flow case (Case 4).

The circulation ratio over the concerned range is still quite larger than that of the typical steam generator without an economizer which has a circulation of about 30 % smaller than that of the KSNP steam generator with an economizer¹.

Since the reciprocal of the circulation ratio is the maximum thermodynamic steam quality within the tube bundle region, the reduced circulation ratio with reducing downcomer flow fraction gives the higher steam quality. In addition, the critical heat flux decreases as the system pressure increases over the pressure range of 700 – 1200 psia² and the resultant critical heat flux is expected to be slightly decreased since the steam pressure increases with the reduced downcomer flow fraction. However, the decrease in the critical heat flux does not drastically reduce the margin for the critical heat flux condition since the circulation ratio as low as 3.0 is considered to have reasonable margin for avoidance of critical heat flux condition³. The circulation ratio is not a unique indication to avoid the problems of the local dryout. Although high circulation ratio implies low quality, it does not necessarily imply high velocities. The velocity distribution is driven by details of tube bundle geometry as well.

3.3. Internal Velocity Distribution

A high velocity flow may cause excessive tube vibration, which results in the wear of tubes. The higher than average velocities potentially exist near the recirculating fluid tube bundle entrance regions. Since excessive flow-induced tube vibration and subsequent wear were reported on a limited number of tubes in the Palo Verde steam generators⁴, a number of design modifications have been made in the KSNP from the YGN 3&4 steam generators to preclude this problem. The flow entering at the cold side recirculating fluid entrance was determined to have caused the tube wear at Palo Verde, therefore several modifications were aimed at reducing the maximum velocity of this flow near the tube lane.

Figure 2 shows the radial velocity distributions at the selected axial locations. The higher velocity is shown in the tube lane region at the tubesheet and the magnitude slightly increases with reducing downcomer feedwater flow fraction. The maximum radial velocity increase is about 4.8 % or less at the tubesheet location compared to the design case. However, at the other locations the maximum radial velocity slightly decreases with reducing feedwater flow fraction. At the tube bundle top location, the magnitudes of the radial velocity are quite higher in the hot side than in the cold side.

The velocities across the tubesheet are concerned with another point of sludge transport. A higher circulation ratio results in higher liquid flow rates at the downcomer entrance at the tubesheet. This allows deeper radial penetration of flow into the bundle and a sustained velocity across the tubesheet to transport sludge to the region of tubes where sludge is removed through the steam generator blowdown system. Therefore the higher velocity is favorable from the point of sludge transport while not favorable from the point of the potential of flow induced tube vibration.

Table 4 shows the maximum radial velocity at the tubesheet in the economizer region. The radial velocity was slightly increased due to increased forced flow with reducing the downcomer feedwater flow. However the higher velocity flow is not expected to cause tube vibration problems at tube bundle entrances at the tubesheet because the tubes have fixed support within the tubesheet and are extremely stiff and resistant to flow induced vibration. In addition the velocity is also quite small compared to the hot side recirculating fluid entrance

velocity. Generally the cold side feedwater entrance to the economizer is the most stable fluid entrance region⁴.

Figure 3 shows the overall axial velocity contour at selected circumferential plane (IX=5). The magnitudes of the local maximum and minimum velocity at the plane slightly decrease with reducing downcomer feedwater flow. However, the overall distribution is nearly the same over all the analyzed cases.

3.4. Internal Void Fraction and Steam Quality

Table 4 shows that the maximum void fraction and steam mass quality at the tube bundle exit location slightly increase with reducing downcomer feedwater flow fraction. The increases are higher at the cold side than the hot side. The maximum local steam mass quality on the plane at the tube bundle exit increases up to 5.28 % and 7.1 % for hot and cold side, respectively, compared to the design case.

Figure 4 shows the void fraction contour on the horizontal plane at the selected axial locations. It is shown that the void fraction in the tube bundle region slightly increases with reducing downcomer feedwater flow fraction. However, the overall distribution is not affected by the downcomer feedwater flow fraction.

Figure 5 shows the axial void fraction contour at the selected axial plane, which is expected to have high void fraction. It is shown that the overall distribution is not affected by the downcomer feedwater flow fraction.

Table 4. ATHOS3 Analyses Result Summary

	Case 1	Case 2	Case 3	Case 4
Downcomer Flow (%)	15.0	10.0	5.1	0.1
Overall Circulation Ratio	3.83	3.81	3.70	3.59
Recirculation Entrance Flow (kg/sec)				
- Hot Side	729.08	716.48	696.23	673.81
- Cold Side	492.74	477.29	430.38	381.33
Max. Tube Lane Radial Velocity (m/sec)				
- Hot Side	1.29	1.332	1.36	1.39
- Cold Side	0.7173	0.759	0.8006	0.8422
Cold Side Recirculation Entrance Radial Velocity (m/sec)	0.1635	0.1585	0.1444	0.08129
Economizer Entrance Radial Velocity (m/sec)	0.6302	0.6671	0.7039	0.7407
Max. Tube Bundle Exit Axial Velocity (m/sec)				
- Hot Side	9.56	9.50	9.399	9.243
- Cold Side	7.754	7.647	7.609	8.696
Max. Tube Bundle Exit Void Fraction				
- Hot Side	0.9554	0.9561	0.9584	0.9605
- Cold Side	0.8131	0.8113	0.8179	0.8234
Max. Tube Bundle Exit Steam Quality				
- Hot Side	0.5371	0.5432	0.5571	0.5719
- Cold Side	0.1907	0.1902	0.1971	0.2037

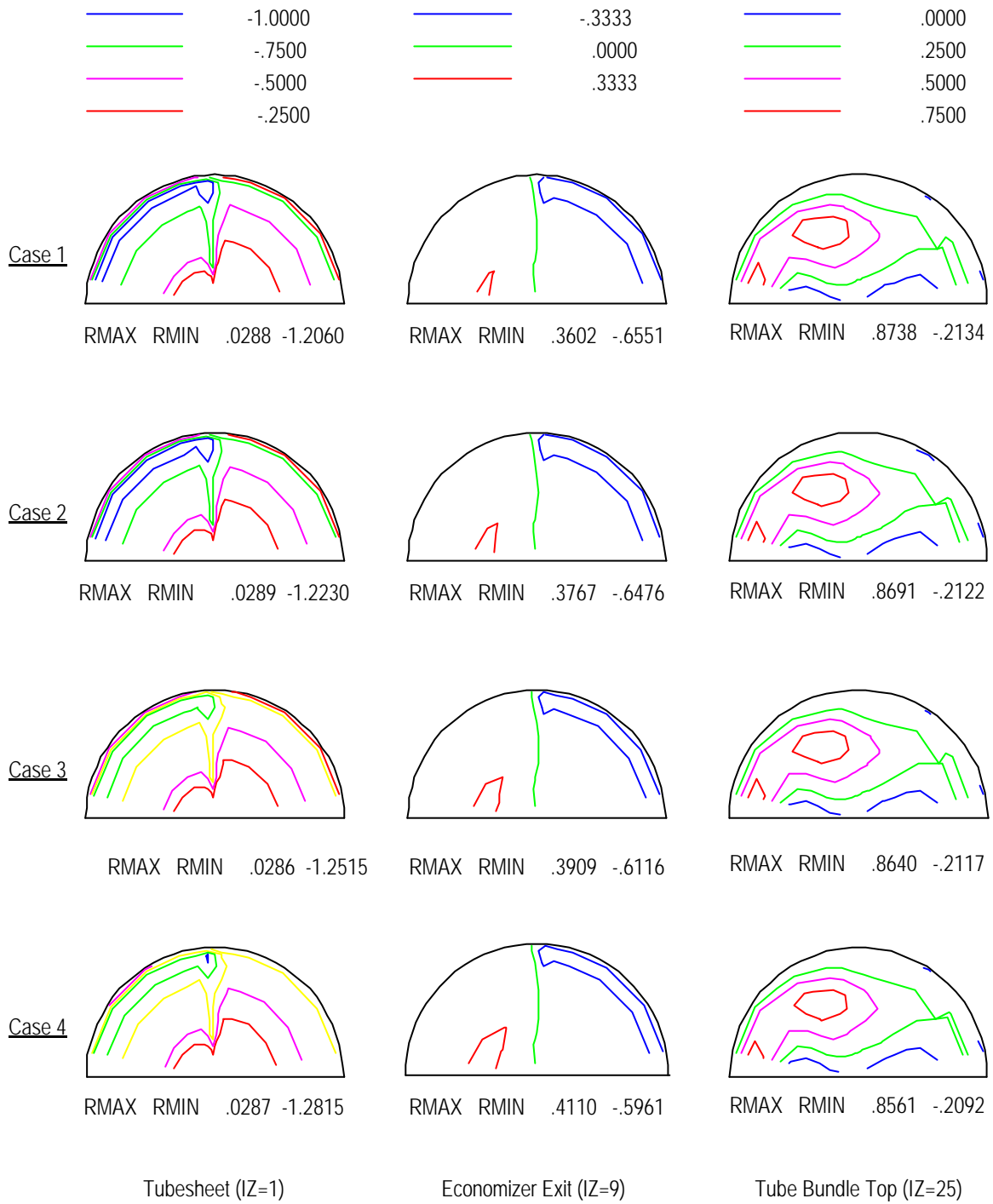


Figure 2. Plane Radial Velocity (m/sec) Distribution

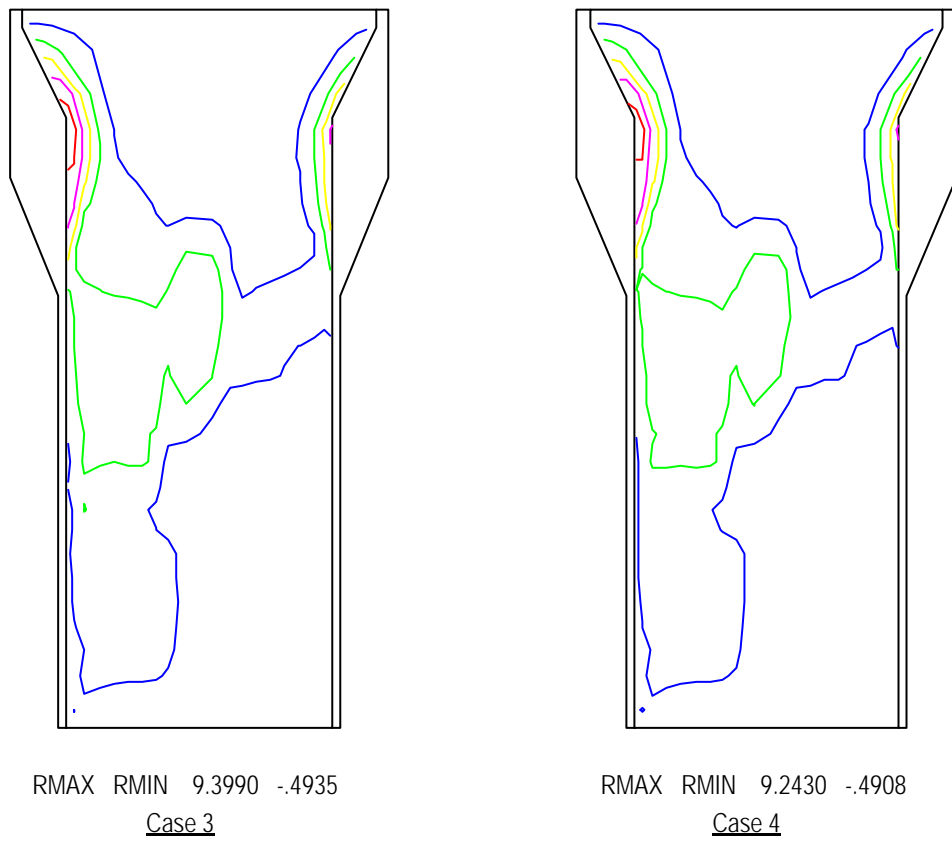
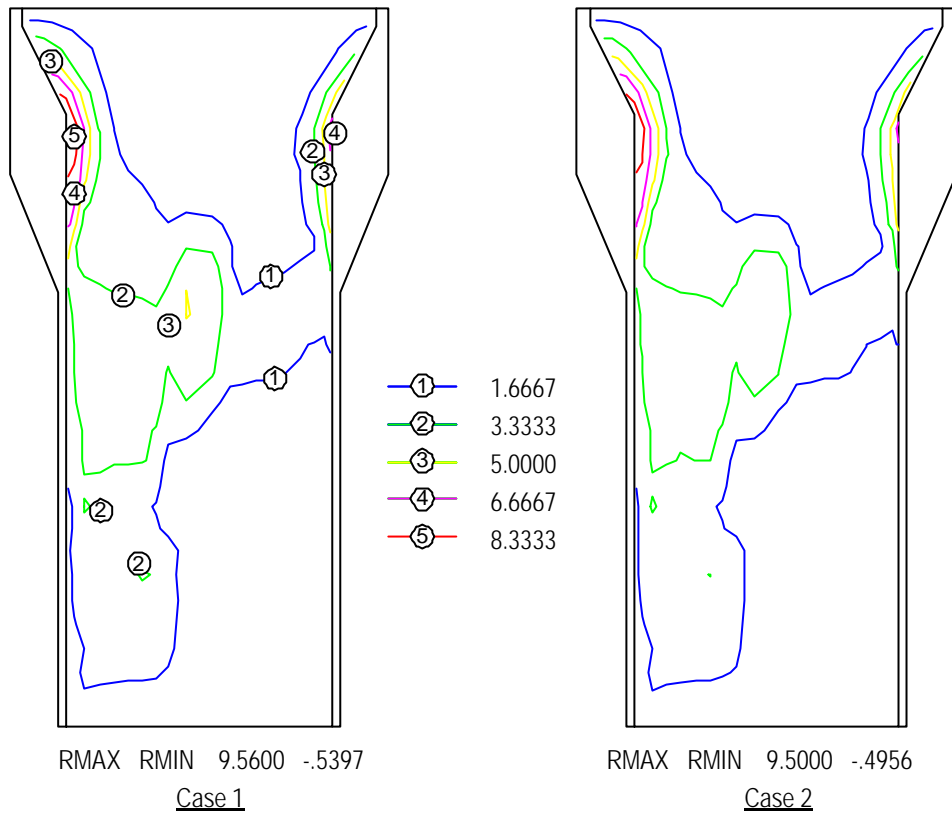


Figure 3. Axial Velocity (m/sec) Distribution (IX=5)

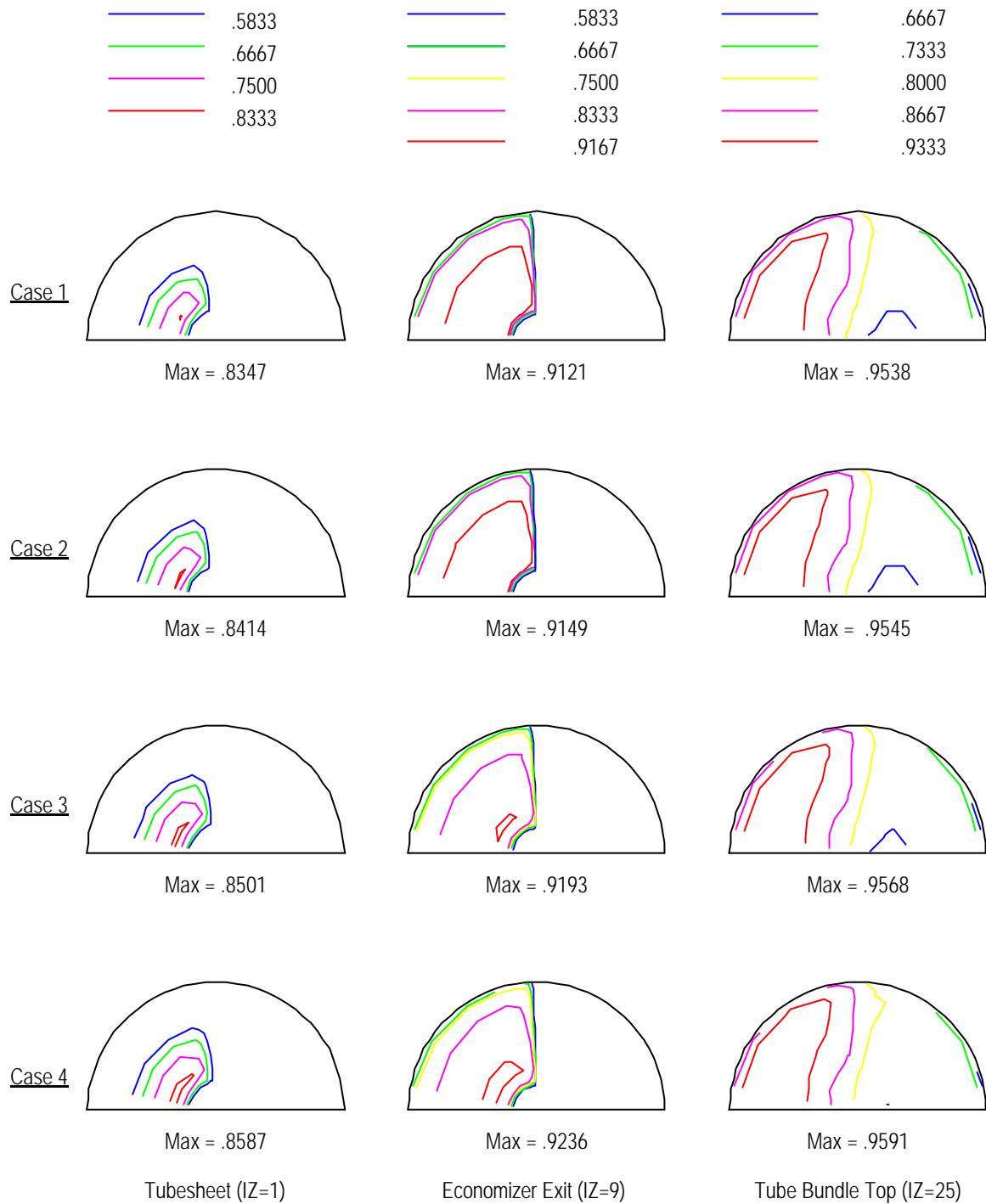


Figure 4. Plane Void Fraction Distribution

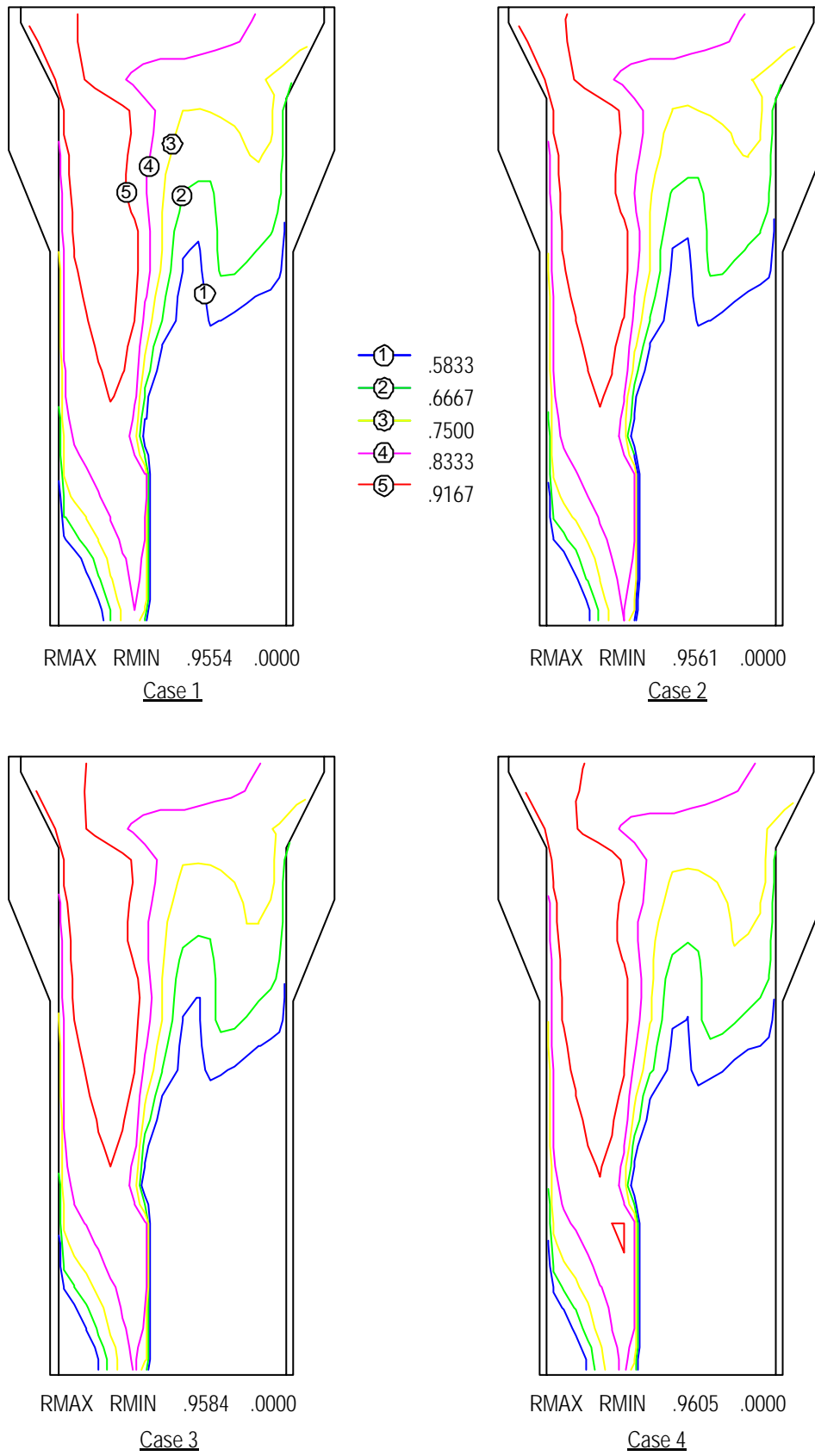


Figure 5. Axial Void Fraction Distribution (IX=1)

4. Conclusion and Recommendation

The analyses show that the steam pressure increase is evaluated to be about 7 psi and the overall circulation ratio decrease about 5.7 % compared to the design case in the almost no feedwater case. From the viewpoint of steam pressure and sludge deposition at the tubesheet, the reduced downcomer feedwater flow fraction gives a little better performance. However, it gives also slight adverse impact on the performance from the standpoint of dryout in the evaporation region. This is the reason why the actual design requires some trade-off between the two aspects of performance. Therefore the downcomer feedwater flow fraction shall be determined to have little effects on the steam generator performance.

In conclusion, the actual slight off-design feedwater flow of up to ± 5 % deviation causes potentially no drastic problem to the axial economizer steam generator performance in terms of circulation ratios, void fractions, steam qualities and internal velocity distributions.

Another aspects of steam generator performance, however, need to be evaluated with reducing the downcomer feedwater flow fraction. One of them is the instability of downcomer water level, which is controlled by the associated control system. A higher system pressure increases the density ratio of steam to liquid and subcooling of downcomer fluid. Forced feedwater flow in the economizer region also has a stabilizing effect. With these features, the increase in quality of the two-phase flow is not expected to cause instability problems. However, the less downcomer flow and lower fluid density effect needs to be evaluated quantitatively on the downcomer water level control performance especially during the transients.

References

- [1] Steam Generator Performance Comparison, Combustion Engineering, Inc., 1984.
- [2] J. G. Collier, *Convective Boiling and Condensation*, McGraw-Hill Int'l Book Company, 1981.
- [3] J. C. Lowry, "Instruction Material for System Designer: Circulation Ratio," 1986.
- [4] N. L. Beard, et. al., "Flow Induced Vibration Analysis Yonggwang Nuclear (YGN) 3/4 Steam Generator Economizer and Lower Tube Bundle Region, CENC-1838, 1988.
- [5] L. M. Barger, et. al, 1400 MWt Steam Generator Descriptive Report, CENC 1754, 1986.
- [6] A. K. Singhal, et. al., "ATHOS3 - A Computer Program for Thermal Hydraulic Analysis of Steam Generators," Volumes 1-3, EPRI NP-2698-CCM, 1982.
- [7] "SAFE - Steam Generator with Axial Flow Economizer," Combustion Engineering, 1976.